Title
Sensitivity Studies of a Standing-Wave Free-Electron Laser

Authors
Rangarajan, G
Sessler, A

Publication Date
1992-06-01

LBL-32463
UC-414

Lawrence Berkeley Laboratory
UNIVERSITY OF CALIFORNIA

Accelerator & Fusion Research Division

Presented at the Workshop on Advanced Accelerator Concepts, Pt. Jefferson, NY, June 14–20, 1992, and to be published in the Proceedings

Sensitivity Studies of a Standing-Wave Free-Electron Laser

G. Rangarajan and A. Sessler

June 1992

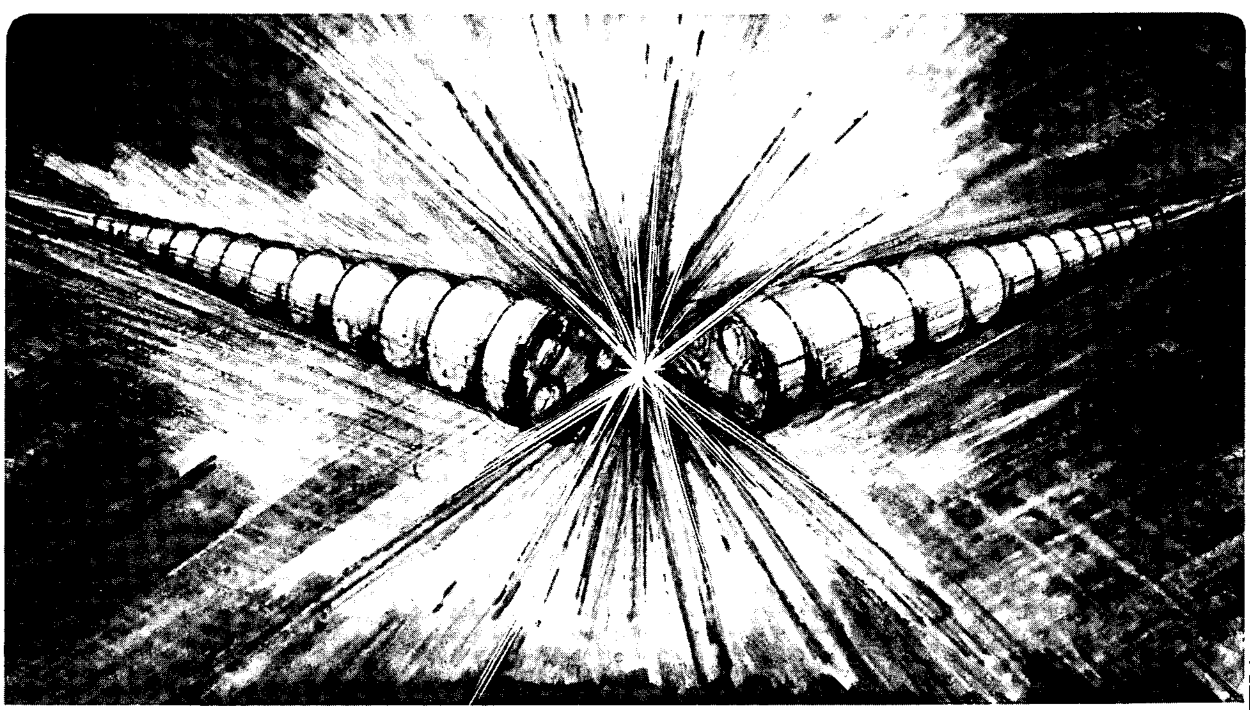

Prepared for the U.S. Department of Energy under Contract Number DE-AC03-76SF00098

DISCLAIMER

LBL-32463
ESG - 197
UC-414

Sensitivity Studies of a Standing-Wave Free-Electron Laser

Govindan Rangarajan and A. Sessler*

Lawrence Berkeley Laboratory, University of California, Berkeley, California 94720

June 1992

*Work supported by the Director, Office of Energy Research, Office of High Energy and Nuclear Physics, Division of High Energy Physics, of the U.S. Department of Energy under Contract No. DE-AC03-76SF00098

SENSITIVITY STUDIES OF A STANDING-WAVE FREE-ELECTRON LASER

Govindan Rangarajan and Andrew M. Sessler

Lawrence Berkeley Laboratory, University of California,

Berkeley, CA 94720

ABSTRACT

A standing-wave free-electron laser (SWFEL) has been proposed for use in a two-beam accelerator (TBA). We modify the previous one-dimensional discrete cavity model of the SWFEL by introducing drifts between cavities. We also vary the input beam energy as a function of the bunch number. In this new model, we obtain a stable equilibrium solution for a well-bunched beam (even after including all nonlinear terms). We obtain analytic expressions characterizing this equilibrium in the limit of small cavity lengths. We study the dependence of fluctuations in signal phase along the device as a function of detuning, input beam energy, beam length, current errors, and initial signal field amplitude. We are able to find an optimized set of parameters for which the output energy changes by less than 3% across the cavities for a 1% detuning. The maximum change in signal phase is less than 0.12 radians.

INTRODUCTION

A "two-beam accelerator" (TBA) has been proposed[1] as a device capable of achieving high accelerating gradients required for the next generation linear colliders. One possible configuration is to use a standing-wave free-electron laser (SWFEL)[2, 3] as a power source for the high gradient structure in a TBA. In this device, irises are placed along the FEL wiggler to form a series of microwave cavities, and induction cells are placed between cavities to reaccelerate the beam (see Figure 1). The standing-wave signal that builds up in the cavities as the beam passes through is coupled to a parallel high-gradient radio-frequency accelerator.

The SWFEL has been studied in some detail in earlier papers[2–5]. In this paper, we study the discrete-cavity model introduced in Ref. [5] in greater detail. First, we introduce a new feature by putting drifts between cavities. Using this additional degree of freedom, we obtain an equilibrium solution for a well-bunched beam. Finally, we perform sensitivity studies around this equilibrium.

EQUILIBRIUM SOLUTION

Previously, an equilibrium solution was obtained[3] for a well-bunched beam in the continuous model of the SWFEL by linearizing the equations of motion. In this section, we obtain a general equilibrium solution (again for a well-bunched beam) using the full nonlinear set of equations. Moreover, this equilibrium solution does not assume small cavity lengths.

We start with the one-dimensional equations of motion in a discrete cavity model of the SWFEL. Since the model and the equations of motion have been discussed in detail elsewhere[5], we restrict ourselves to a brief description. The discrete-cavity model takes into account time-of-flight effects within the cavity and applies the reacceleration field only between cavities, where the ponderomotive force is absent. As in previous SWFEL models, only a single signal frequency is considered.

Within a cavity, we solve the conventional wiggle-averaged FEL equations. Denoting the particle phase $(k_s + k_w)z - \omega_s t$ by θ_j, the particle energy by γ_j, and taking $\tilde{z}$ to be the independent variable, the equations are given as follows

$$\frac{d\theta_j}{d\tilde{z}} = k_w + k_s - \frac{\omega_s}{c} - \frac{\omega_s}{2c\gamma_j^2}\left[1 + \frac{a_w^2}{2} - 2D_x a_w a_s \cos(\theta_j + \phi)\right], \qquad (1)$$

$$\frac{d\gamma_j}{d\tilde{z}} = -D_x \frac{\omega_s}{c} \frac{a_w}{\gamma_j} a_s \sin(\theta_j + \phi), \tag{2}$$

$$\frac{d\hat{a}}{d\tilde{z}} = i\eta \langle \frac{\exp(-i\theta_j)}{\gamma_j} \rangle. \tag{3}$$

Here a_s and ϕ denote the field amplitude and field phase respectively. The coupling coefficient D_x is given by

$$D_x = [J_o(\xi) - J_1(\xi)]/2, \tag{4}$$

where $\xi = \omega_s a_w^2/(8ck_w\gamma_j^2)$. The coefficient η is given by

$$\eta = \frac{8\pi}{hw} \frac{eI_b}{m_e c^3} \frac{D_x a_w}{k_s}. \tag{5}$$

The full interaction of the electron beam with the SWFEL structure can be represented symbolically by the following recursion relations:

$$\theta_{k,l} = \theta_{k,l-1} + F_\theta(\theta_{k,l-1}, \gamma_{k,l-1}, (a_s)_{k,l-1}, \phi_{k,l-1}), \tag{6}$$

$$\gamma_{k,l} = \gamma_{k,l-1} + F_\gamma(\theta_{k,l-1}, \gamma_{k,l-1}, (a_s)_{k,l-1}, \phi_{k,l-1}) + \Delta\gamma_{k,l-1}, \tag{7}$$

$$(a_s)_{k,l} = (a_s)_{k-K',l} + F_a(\theta_{k-K',l}, \gamma_{k-K',l}, (a_s)_{k-K',l}, \phi_{k-K',l}), \tag{8}$$

$$\phi_{k,l} = \phi_{k-K',l} + F_\phi(\theta_{k-K',l}, \gamma_{k-K',l}, (a_s)_{k-K',l}, \phi_{k-K',l}). \tag{9}$$

Here, θ and γ are n-vectors where n is the number of particles in a bunch. The quantities $\theta_{k,l}$, $\gamma_{k,l}$, $(a_s)_{k,l}$, and $\phi_{k,l}$ represent values of θ, γ, a_s, and ϕ for the kth bunch at the beginning of the lth cavity. The functions F_θ, F_γ, F_a, and F_ϕ represent the FEL interaction within a cavity. The quantity $\Delta\gamma_{k,l}$ is the reacceleration field for kth bunch after the lth cavity. The bunch skip factor K' is equal to the number of bunches that pass through by the time the forward traveling radiation field makes a round trip within a cavity (see Ref. [5] for further details):

$$K' \approx 2L_c/\lambda_s. \tag{10}$$

Here, L_c is the length of the cavity and the signal wavelength λ_s is the average separation between electron bunches.

We are now in a position to derive an equilibrium solution. In a discrete-cavity model, an equilibrium solution is a solution where all the cavities behave in an identical fashion. The equilibrium is derived for a well-bunched beam i.e. θ and γ in Eqs. (6) and (7) are now scalars representing the average particle phase and average energy of an electron bunch. First, we modify the discrete-cavity model by introducing a drift space after each cavity. All drift spaces are taken to be identical to one another. The drift space is designed as follows. Consider the first bunch of electrons traversing the first cavity. By the time it exits the cavity, its θ would have changed by a finite amount, say $\Delta\theta$. The drift space is designed such that it exactly compensates for this change. That is, the particle phase changes by an amount $-\Delta\theta$ when passing through the drift. When the drift spaces are incorporated into our model, Eq. (6) is modified as follows

$$\theta_{k,l} = \theta_{k,l-1} + F_\theta(\theta_{k,l-1}, \gamma_{k,l-1}, (a_s)_{k,l-1}, \phi_{k,l-1}) - \Delta\theta. \tag{11}$$

Since we cannot change the drift length from bunch to bunch we have to ensure that all bunches undergo the same change $\Delta\theta$ in the first cavity. Only then will the θ correction scheme work for all bunches. This is achieved by choosing the input energy $\gamma_{k,1}$ such that the following condition is satisfied

$$F_\theta(\theta_{k,1}, \gamma_{k,1}, (a_s)_{k,1}, \phi_{k,1}) = \Delta\theta \qquad \forall\ k. \tag{12}$$

Next, we choose the reaccleration field such that it restores the energy lost by a bunch in a cavity i.e.

$$\Delta\gamma_{k,l} = -F_\gamma(\theta_{k,l}, \gamma_{k,l}, (a_s)_{k,l}, \phi_{k,l}) \qquad \forall\ k \text{ and } l. \tag{13}$$

Finally, the input radiation field amplitude and phase are taken to be the same for all cavities (i.e. $(a_s)_{1,l}$ and $\phi_{1,l}$ are independent of l). Once we satisfy all these conditions, we obtain a cavity-independent equilibrium. This can be seen as follows. From Eqs. (7) and (13), we find that $\gamma_{k,l} = \gamma_{k,1} \; \forall \; k$. From Eqs. (11) and (12), we find that $\theta_{k,2} = \theta_{k,1} \;\; \forall \; k$. Using these two equalities and the fact that $(a_s)_{1,2} = (a_s)_{1,1}$ and $\phi_{1,2} = \phi_{1,1}$, we find from Eqs. (8) and (9) that $(a_s)_{k,2} = (a_s)_{k,1}$ and $\phi_{k,2} = \phi_{k,1}$ for all k. Thus, the first two cavities behave in an identical fashion. Repeating this argument, one can easily show that the behaviour of any dynamical variable is independent of l. Since the drift spaces compensate for the change in θ and the reacceleration field compensates for the change in γ, the electron bunches see exactly the same initial conditions in all the cavities. Therefore, the resulting solution of the FEL equations is identical for all cavities.

The above equilibrium solution only fixes the input value of one variable – γ. The input values of the remaining variables are determined as follows. It is well known that multi-particle stability arguments favour a value of the equilibrium ponderomotive phase ψ $(= \theta + \phi)$ close to zero. However, other considerations like sensitivity to detuning (see the next section for further details) favour a ψ close to $\pi/2$. As a compromise, we typically take ψ to be a constant equal to $\pi/3$. This fixes $\theta_{k,1}$:

$$\theta_{k,1} = -\phi_{k,1} + \pi/3. \tag{14}$$

We still have to fix $\phi_{1,1}$ and $(a_s)_{1,1}$. Usually, $\phi_{1,1}$ is taken to be zero. To reduce sensitivity to detuning (see next section), $(a_s)_{1,1}$ is taken to be as high as is practically possible.

For long cavities, it is not possible to give an analytic expression for the equilibrium solution. However, this is possible for very short cavities where the continuous model is valid. This is the subject of our next subsection.

A. Equilibrium Solution in the Continuous Model

The continuous model is obtained by taking the cavity length to be so short that the Euler formula can be used to integrate the FEL equations within a cavity. From Eqs. (1)–(3) and (6)–(9), we obtain the following results (assuming a well-bunched beam)

$$F_\theta/L_c = k_w + k_s - \frac{\omega_s}{c} - \frac{\omega_s}{2c\gamma^2}\left[1 + \frac{a_w^2}{2} - 2D_x a_w a_s \cos(\theta+\phi)\right], \tag{15}$$

$$F_\gamma/L_c = -D_x \frac{\omega_s}{c}\frac{a_w}{\gamma} a_s \sin(\theta+\phi), \tag{16}$$

$$F_a/L_c = \eta \frac{\sin(\theta+\phi)}{\gamma}, \tag{17}$$

$$F_\phi/L_c = \eta \frac{\cos(\theta+\phi)}{a_s\gamma}. \tag{18}$$

Substituting the above expressions into Eqs. (7)–(9) and (11), we can convert them into the following differential equations:

$$\frac{d\theta}{dz} = k_w + k_s - \frac{\omega_s}{c} - \frac{\omega_s}{2c\gamma^2}\left[1 + \frac{a_w^2}{2} - 2D_x a_w a_s \cos(\theta+\phi)\right] - \overline{\Delta\theta}, \tag{19}$$

$$\frac{d\gamma}{dz} = -D_x \frac{\omega_s}{c}\frac{a_w}{\gamma} a_s \sin(\theta+\phi) - \frac{eE_z}{m_e c^2}, \tag{20}$$

$$\frac{\partial a_s}{\partial s} = \eta' \frac{\sin(\theta+\phi)}{\gamma}, \tag{21}$$

$$\frac{\partial \phi}{\partial s} = \eta' \frac{\cos(\theta+\phi)}{a_s\gamma}. \tag{22}$$

Here, z denotes the longitudinal distance along the device, E_z is the external reacceleration field, and s denotes the normalized distance from the beam head. The quantity $\overline{\Delta\theta}$ is the change in θ per unit length for the first electron bunch:

$$\overline{\Delta\theta} = \frac{D_x a_w \omega_s}{c\gamma_r^2} a_s(s=0)\cos\psi(s=0). \tag{23}$$

Here we have assumed that the first electron bunch comes in with the resonant energy γ_r and the ponderomotive phase $\psi(s=0)$. The field coupling coefficient η' is given as follows:

$$\eta' = \eta L_b/2, \tag{24}$$

where L_b is the length of the beam.

For an equilibrium solution, we require θ and γ to be z-independent. Denoting the equilibrium values by a subscript 0, we obtain the following result from Eq. (19):

$$\gamma_0^2(s) = \frac{\left[\frac{\omega_s}{2c}\left(1+\frac{a_w^2}{2}\right) - \frac{D_x a_w \omega_s}{c} a_{s0}(s)\cos\psi_0(s)\right]}{(k_w + k_s - \omega_s/c - \overline{\Delta\theta})}. \tag{25}$$

Typically, $\overline{\Delta\theta} \ll (k_w + k_s - \omega_s/c)$. Therefore, we get

$$\gamma_0^2(s) \approx \gamma_r^2 - \frac{D_x a_w \omega_s a_{s0}(s)\cos\psi_0(s)}{c(k_w + k_s - \omega_s/c)}. \tag{26}$$

From Eq. (20), we get

$$\frac{eE_z}{m_e c^2} = -D_x a_w \frac{\omega_s}{c}\frac{a_{s0}(s)\sin\psi_0(s)}{\gamma_0(s)}. \tag{27}$$

Before we can proceed further, we have to fix $\theta_0(s)$, which is a free parameter. To simplify calculations, we choose it as follows [cf. Eq. (14)]

$$\theta_0(s) = -\phi_0(s) + \pi/3. \tag{28}$$

That is, the equilibrium ponderomotive phase ψ_0 is a constant independent of s. Now, we can solve for $a_{s0}(s)$ and $\phi_0(s)$ from Eqs. (21) and (22). Assuming a constant current i.e.

$$\eta'(s) = \eta'_0, \tag{29}$$

we get the following expression for $a_{s0}(s)$ and $\phi_0(s)$:

$$a_{s0}(s) \approx a_{s0}(0) + \frac{\eta'_0 \sin\psi_0}{\gamma_r} s, \tag{30}$$

$$\phi_0(s) \approx \phi_0(0) + \cot\psi_0 \;\ln\left[1 + \frac{\eta'_0 \sin\psi_0}{\gamma_r a_{s0}(0)} s\right]. \tag{31}$$

By substituting these results into Eqs. (26)–(28), we can obtain analytic expressions for all quantities of interest. Similar expressions can be obtained for the linearly ramped current case.

NUMERICAL RESULTS

In this section, we numerically study the SWFEL model described in the previous section. We perform sensitivity studies around the new equilibrium described in Eqs. (12) — (14). First, we study a short cavity case (where $L_c = \lambda_s$ = 1.83 cm) and then a long cavity case (where L_c = 14.7 cm). The simulation parameters are listed in Table 1. We set the initial signal level $|a_s(0)|$ by assuming some input power per unit length P_{in} and balancing this with cavity-wall losses, specified by an assumed cavity Q. The average beam current has been chosen to give an output energy per unit length of 10 J/m. For multiparticle simulations, we use a 1% spread in γ and a 10% spread in θ. Typically, we use 200 simulation particles.

A. Studies using short cavities

In this subsection, we numerically study a SWFEL using short FEL cavities. Length of each cavity is taken to be λ_s. In this case, our model of the SWFEL reduces to the continuous model introduced earlier[3] (other than for the drifts). All studies are performed around the equilibrium solution described in the previous section. This equilibrium is achieved in our numerical simulations by varying the input beam energy according to Eq. (25) and by fixing the drift lengths using Eq. (23). For the parameters given in Table 1, the variation in beam energy from the head to the tail of the beam is less than 4% (for a constant current, the input energy decreases linearly [cf. Eqs. (26) and (30)]). The reacceleration field compensates for the average energy lost in the previous cavity.

First, we study the effects of detuning on the output microwave energy per unit length W_{out} and signal phase ϕ. Detuning is achieved by offsetting the input energies of all particles by a fixed fraction $\Delta\gamma_0/\gamma_0$. Figure 2 shows the effects of 0, 0.5, and 1 percent detuning on W_{out} and ϕ for a well-bunched beam. As expected, for zero detuning we get a perfect equilibrium solution. In this case, we have verified that the analytic formulas given in Eqs. (30) and (31) agree quite well with the numerical simulations. However, for non-zero detuning, the amplitude of phase fluctuations exceeds the required tolerances (the maximum change in signal phase, $(\Delta\phi)_{max}$, needs to be less than 0.2 radians for the TBA to operate properly[3]).

We can get around this problem as follows. From earlier studies[4], we know that most of the phase ripple is introduced in the early part of the beam where $|a_0(s)|$ is small. This can be seen heuristically as follows. By linearizing around the equilibrium solution, we obtain the following dependence of the phase fluctuation amplitude ϕ_1 on the detuning $\Delta\gamma_0/\gamma_0$:

$$\frac{\partial\phi_1}{\partial s} \approx -\eta' \frac{\cos\psi_0}{a_{s0}\gamma_0} \frac{\Delta\gamma_0}{\gamma_0}. \tag{32}$$

Thus, ϕ_1 builds up in amplitude when $a_{s0}(s)$ is small i.e. when s is small. Therefore, we can reduce the buildup by modifying the input beam energy as follows:

$$\gamma_{in}(s) = \gamma_0(s)\left[1 + \frac{\Delta\gamma_0}{\gamma_0}\frac{1}{1+\exp(\frac{s-s_0}{\delta s})}\right], \tag{33}$$

where we set $s_0/L_b = 0.2$ and $\delta s/L_b = 0.05$. With this modification, the magnitudes of phase fluctuations are within tolerance limits (cf. Figure 3). We repeat the calculation using many particles. In this case, the average input γ is given by Eq. (33). Again, the phase fluctuations are manageable (cf. Figure 4). These findings show that, in order to meet the tolerances on ϕ fluctuations, the beam energy needs to be near γ_0 for at most only the first 20% of the beam. This modulation of γ_0 should be achievable in practice beacuse of reduced beam loading near the head of the beam.

The above argument also suggests that we can reduce ϕ fluctuations by increasing the input power (thereby increasing $a_{s0}(0)$). This is found to be true.

However, modifying the input beam energy as shown in Eq. (33) works better than increasing P_{in}. And once Eq. (33) is implemented, any increase in P_{in} has little effect. Therefore, in all simulations that follow, we will use γ_{in} as given by Eq. (33).

Using Eq. (32), we can justify the choice of $\pi/3$ for the equilibrium value of ψ_0. We see that the magnitude of ϕ_1 fluctuations is reduced as $\psi_0 \rightarrow \pi/2$. However, multiparticle stability requirements favour a ψ_0 value close to zero. Using numerical simulations, we find that $\psi_0 = \pi/3$ is a good compromise value.

Equation (32) also suggests that the magnitude of phase fluctuations can be reduced by going to a higher input γ. A higher input γ is achieved by keeping ω_s and a_w constant and increasing λ_w. To keep the output power level constant, we need to increase beam current as we increase γ. Figure 5 shows the variation of $(\Delta\phi)_{max}$ as a function of input γ for a 1% detuning. We see a significant reduction in $(\Delta\phi)_{max}$ as the input beam energy increases thus verifying the above hypothesis. However, we can not increase the input beam energy beyond a certain point. The initial cost of generating a very high energy beam would become too high (since the efficiency of a TBA decreases with a higher input beam energy) and the additional requirement of a higher beam current would lead to beam breakup problems. Keeping these considerations in mind, we have proposed an optimized set of parameters in Table 1. For these parameters, $(\Delta\phi)_{max}$ is only 0.12 radians for a 1% detuning.

If one increases the wiggler strength a_w while keeping the input γ fixed, $(\Delta\phi)_{max}$ increases. On the other hand, if λ_w is held fixed and a_w is increased (thus increasing input γ also), $(\Delta\phi)_{max}$ remains approximately constant. This is because increasing a_w increases $(\Delta\phi)_{max}$ whereas increasing γ decreases $(\Delta\phi)_{max}$. Therefore, if both are increased, these two effects cancel one another leading to a constant $(\Delta\phi)_{max}$.

Further, we find that a 2% error in beam current has no significant effect on $(\Delta\phi)_{max}$. Neither does a random 1% error in the magnitude of reacceleration field. For very short beams, $(\Delta\phi)_{max}$ tends to be higher. However, once the beam length exceed a critical value (~40 cms), $(\Delta\phi)_{max}$ settles down to a stable value independent of L_b.

B. Studies using long cavities

In this subsection, we perform sensitivity studies around the equilibrium solution using cavities of length 14.7 cm. This is done to check if long cavity lengths lead to new physical effects not present in the continuous model. We find that there are no significant deviations from the results obtained for the continuous model. As in the continuous model, specifying γ_{in} according to Eq. (33), increasing input power, and increasing input γ all help reduce ϕ fluctuations (see Figures 6 and 7). However, there is one case where the long cavity case appears (at first glance) to differ significantly from the continuous model. For a cavity of length 14.7 cm, we find that the beam length has to be greater than 300 cm before $(\Delta\phi)_{max}$ settles down to a stable value independent of L_b. This apparent discrepancy goes away when one analyses the situation more closely. If we look at the last bunch in a beam of length L_b, out of the L_b/λ_s bunches that have preceeded it, it can interact only with $L_b/2L_c$ bunches [cf. Eq. (10)]. And this number is approximately equal for both the continuous model (where $L_c = 1.8$ cm and critical beam length is ~40 cm) and the long cavity case (where $L_c =$ 14.7 cm and critical beam length is ~300 cm).

Finally, we find results similar to ones obtained above even if we increase the cavity length further — to 22 cm and further to 38.5 cm.

SUMMARY

We have developed a discrete cavity model of a SWFEL incorporating drifts in between cavities. A new equilibrium solution was found for this model (when the electrons are well bunched) by varying the input beam energy as a function of bunch number. We performed sensitivity studies around this new equilibrium. Remarkably similar sensitivities were observed irrespective of the cavity length. Keeping the beam energy close to the equilibrium value for the initial part of the beam was found to decrease sensitivity to detuning by a significant amount. A higher value of the input beam energy also led to decreased sensitivity. Errors in beam current and reacceleration field magnitudes did not lead to any significant increase in signal phase fluctuations. Using these results, we have been able to find a set of parameters for which the SWFEL has a tolerable sensitivity to detuning. One result that should help in future studies is the observation that the continuous model and the discrete cavity model behave in a similar fashion. Therefore, one needs to study only the more tractable continuous model in great detail.

ACKNOWLEDGMENTS

This work was supported by the U.S. Department of Energy under contracts DE-AC03-76SF00098 (LBL) and W-7405-ENG-48 (LLNL). We would like to thank Dr. Bill Sharp and Dr. David Whittum for useful discussions.

REFERENCES

[1] A. M. Sessler, in *Laser Acceleration of Particles*, edited by P. J. Channell (AIP, New York, 1982), p.154.

[2] W. M. Sharp, A. M. Sessler, D. H. Whittum, and J. S. Wurtele, Proc. 1990 Linear Accelerator Conference, Albuquerque, LA-12004-C Conference, 656 (1991).

[3] A. M. Sessler, D. H. Whittum, W. M. Sharp, M. A. Makowski, and J. S. Wurtele, Nucl. Instr. and Meth. A306, 592 (1991).

[4] W. M. Sharp, G. Rangarajan, A. M. Sessler, and J. S. Wurtele, Proc. SPIE Conference 1407, 535 (1991).

[5] G. Rangarajan, A. Sessler, and W. M. Sharp, Proc. 12th Int. Free Electron Laser Conf., Nucl. Instr. and Meth. A (1992) (in press).

TABLES

TABLE I. Simulation parameters for the standing-wave FEL

Parameter	Nominal value	Optimized value
average beam current (I_b)	1.8 kA	3.2 kA
beam length (L_b)	440.0 cm	440.0 cm
resonant energy (γ_r)	16.4	32.2
wiggler strength (a_w)	1.4	1.4
wiggler wavelength (λ_w)	37 cm	39.3 cm
wiggler length (L_w)	40 m	40 m
waveguide height (h)	3 cm	3 cm
waveguide width (w)	10 cm	10 cm
signal frequency ($\omega_s/2\pi$)	17.1 GHz	17.1 GHz
cavity quality (Q)	10^4	10^4
input power (P_{in})	8 kW/m	8 kW/m
output energy (W_{out})	10 J/m	10 J/m

FIGURES

FIG. 1. Conceptual layout of one section of a standing-wave TBA.

FIG. 2. Single-particle simulations of the continuous model for the nominal parameters given in Table 1. Three values of $\Delta\gamma_0/\gamma_0$ are studied. Figure 2a shows the output energy per unit length W_{out} and Figure 2b shows the wave phase ϕ as functions of z.

FIG. 3. Single-particle simulations of the continuous model for the nominal parameters given in Table 1. Three values of $\Delta\gamma_0/\gamma_0$ are studied. In these simulations, $\Delta\gamma_0/\gamma_0$ is zero near the beam head and increases to the indicated value (0.5% or 1.0%) near $s/L_b = 0.2$. Figure 3a shows the output energy per unit length W_{out} and Figure 3b shows the wave phase ϕ as functions of z.

FIG. 4. Multi-particle simulations of the continuous model for the nominal parameters given in Table 1. Three values of $\Delta\gamma_0/\gamma_0$ are studied. In these simulations, $\Delta\gamma_0/\gamma_0$ is zero near the beam head and increases to the indicated value (0.5% or 1.0%) near $s/L_b = 0.2$. Figure 4a shows the output energy per unit length W_{out} and Figure 4b shows the wave phase ϕ as functions of z.

FIG. 5. Single-particle simulations of the continuous model for the nominal parameters given in Table 1. This figure displays the variation of $(\Delta\phi)_{max}$ as a function of the input beam energy γ_0 for $\Delta\gamma_0/\gamma_0 = 1\%$. The input beam energy is varied by

keeping ω_s and a_w fixed and varying only λ_w.

FIG. 6. Single-particle simulations of the discrete cavity model (L_c = 14.7 cm) for the nominal parameters given in Table 1. Three values of $\Delta\gamma_0/\gamma_0$ are studied. In these simulations, $\Delta\gamma_0/\gamma_0$ is zero near the beam head and increases to the indicated value near s/L_b = 0.2. Figure 6a shows the output energy per unit length W_{out} and Figure 6b shows the wave phase ϕ as functions of z.

FIG. 7. Single-particle simulations of the discrete cavity model (L_c = 14.7 cm) for the nominal parameters given in Table 1. This figure displays the variation of $(\Delta\phi)_{max}$ as a function of the input beam energy γ_0 for $\Delta\gamma_0/\gamma_0$ = 1%. The input beam energy is varied by keeping ω_s and a_w fixed and varying only λ_w.

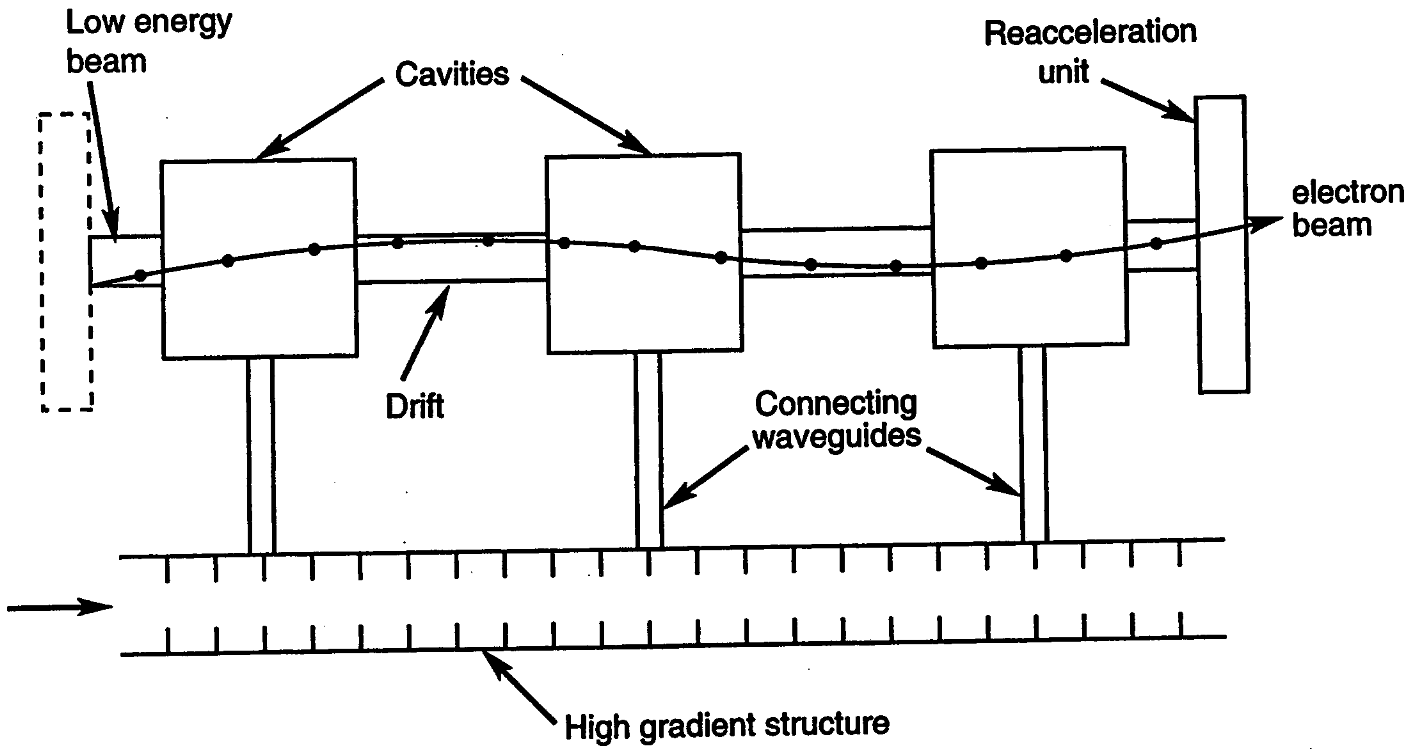
Low energy
beam
Cavities
Reacceleration
unit
electron
beam
Drift
Connecting
waveguides
High gradient structure

Fig. 1

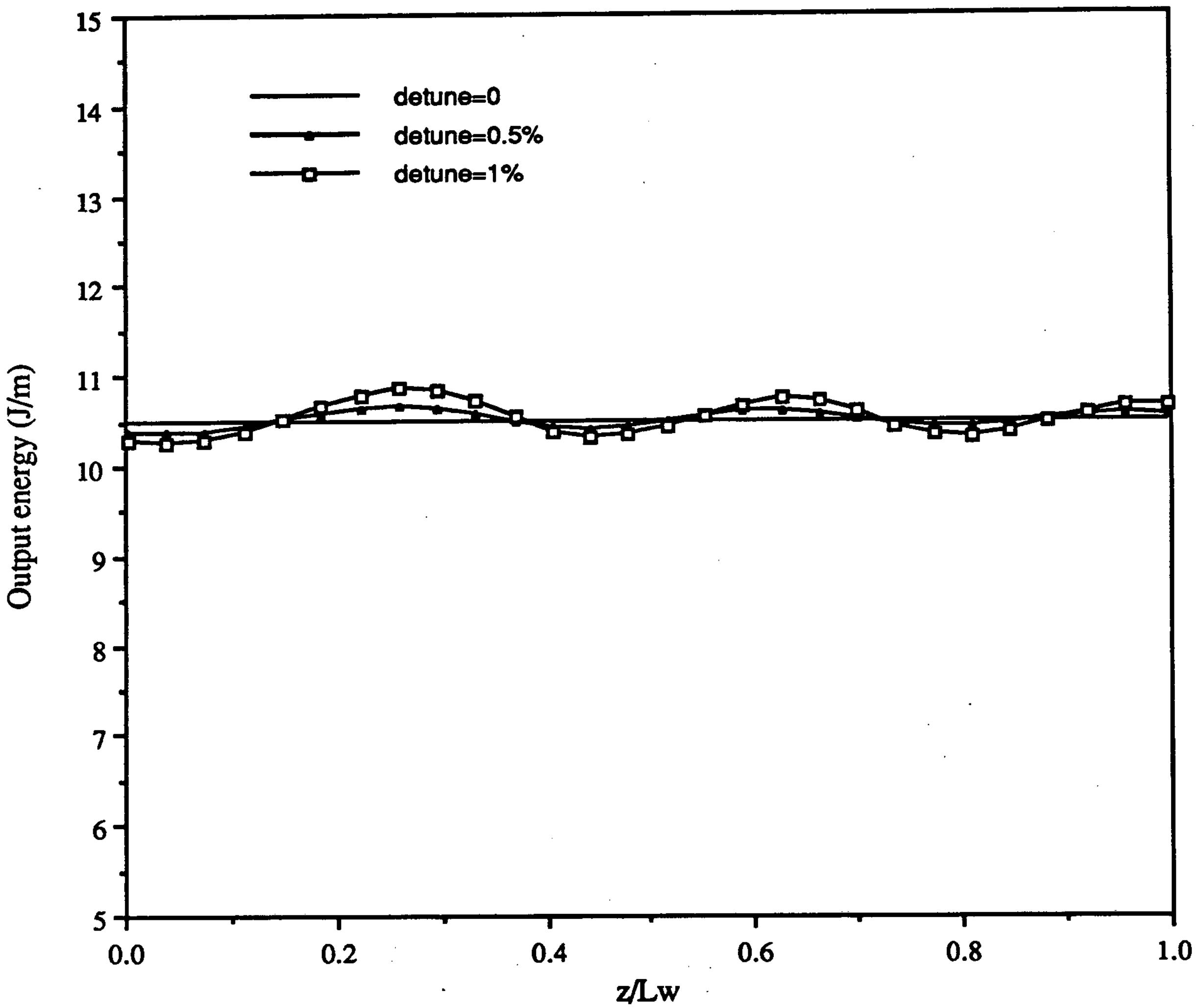
detune=0
detune=0.5%
detune=1%
Output energy (J/m)
15
14
13
12
11
10
9
8
7
6
5
0.0
0.2
0.4
0.6
0.8
1.0
z/Lw

Fig. 2a

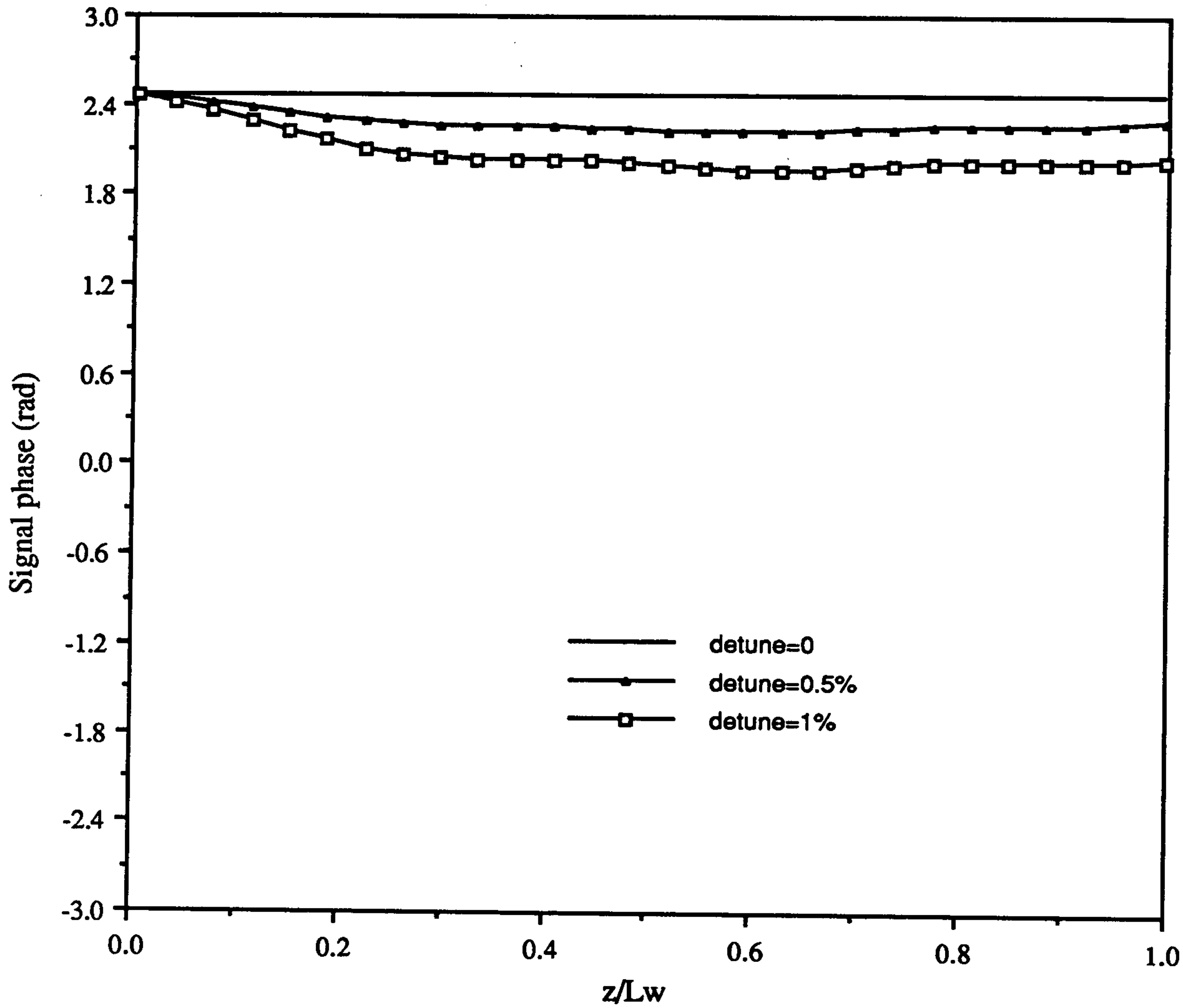
3.0
2.4
1.8
1.2
0.6
0.0
-0.6
-1.2
-1.8
-2.4
-3.0
Signal phase (rad)
0.0
0.2
0.4
0.6
0.8
1.0
z/Lw
detune=0
detune=0.5%
detune=1%

Fig. 2b

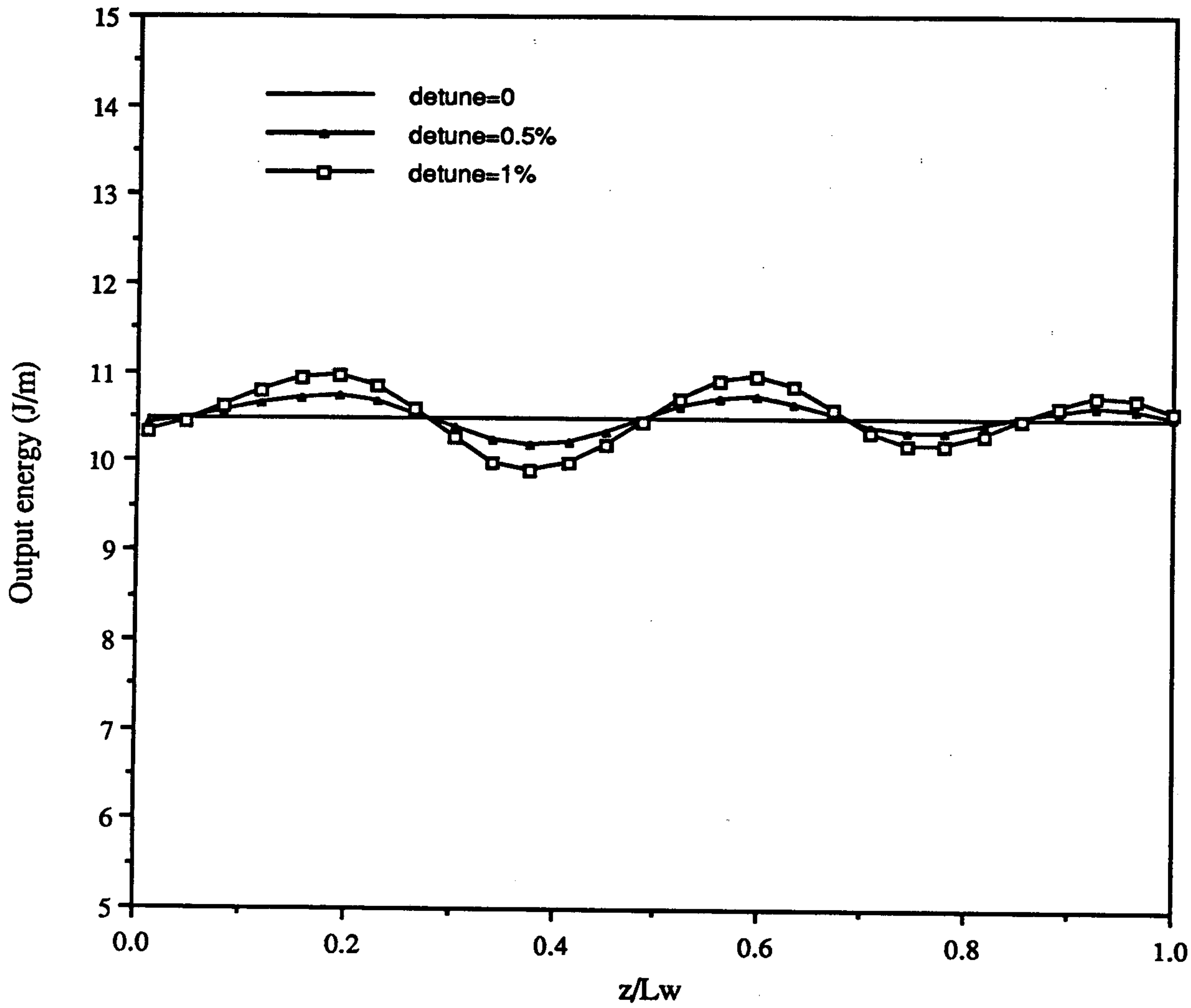

detune=0
detune=0.5%
detune=1%
Output energy (J/m)
z/Lw
5
6
7
8
9
10
11
12
13
14
15
0.0
0.2
0.4
0.6
0.8
1.0

Fig. 3a

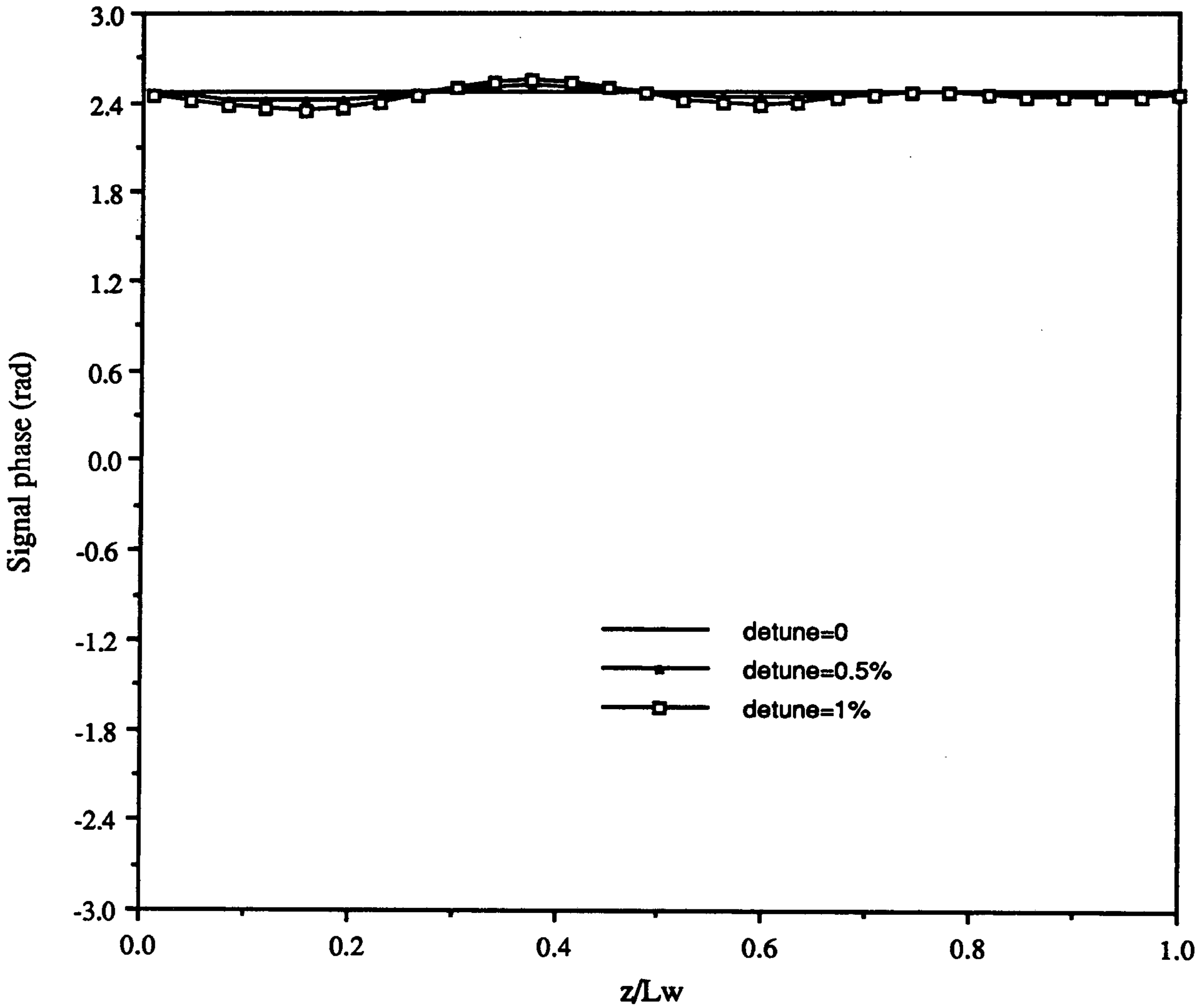
3.0
2.4
1.8
1.2
0.6
0.0
-0.6
-1.2
-1.8
-2.4
-3.0
Signal phase (rad)
0.0
0.2
0.4
0.6
0.8
1.0
z/Lw
detune=0
detune=0.5%
detune=1%

Fig. 3b

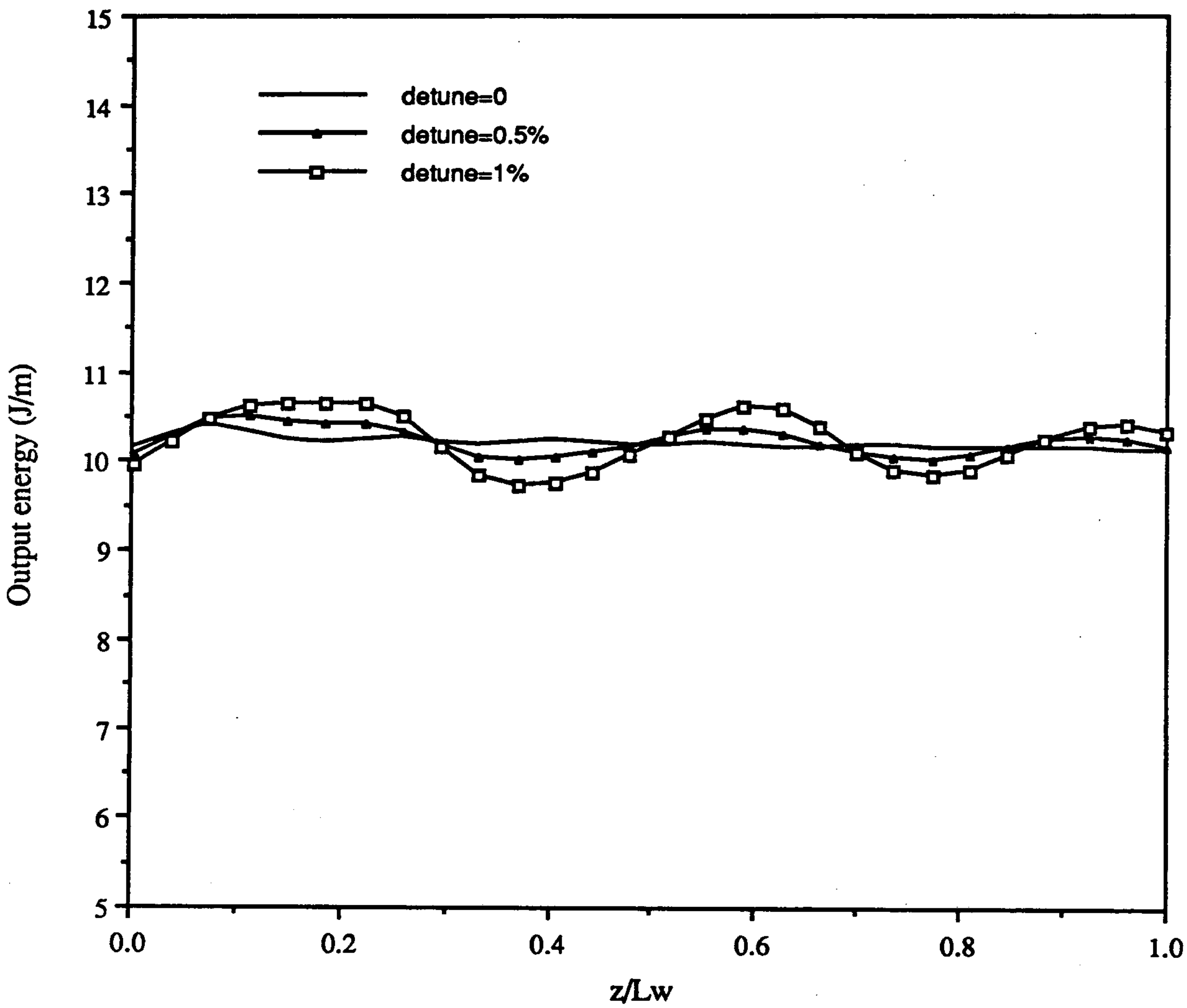
detune=0
detune=0.5%
detune=1%
Output energy (J/m)
z/Lw
15
14
13
12
11
10
9
8
7
6
5
0.0
0.2
0.4
0.6
0.8
1.0

Fig. 4a

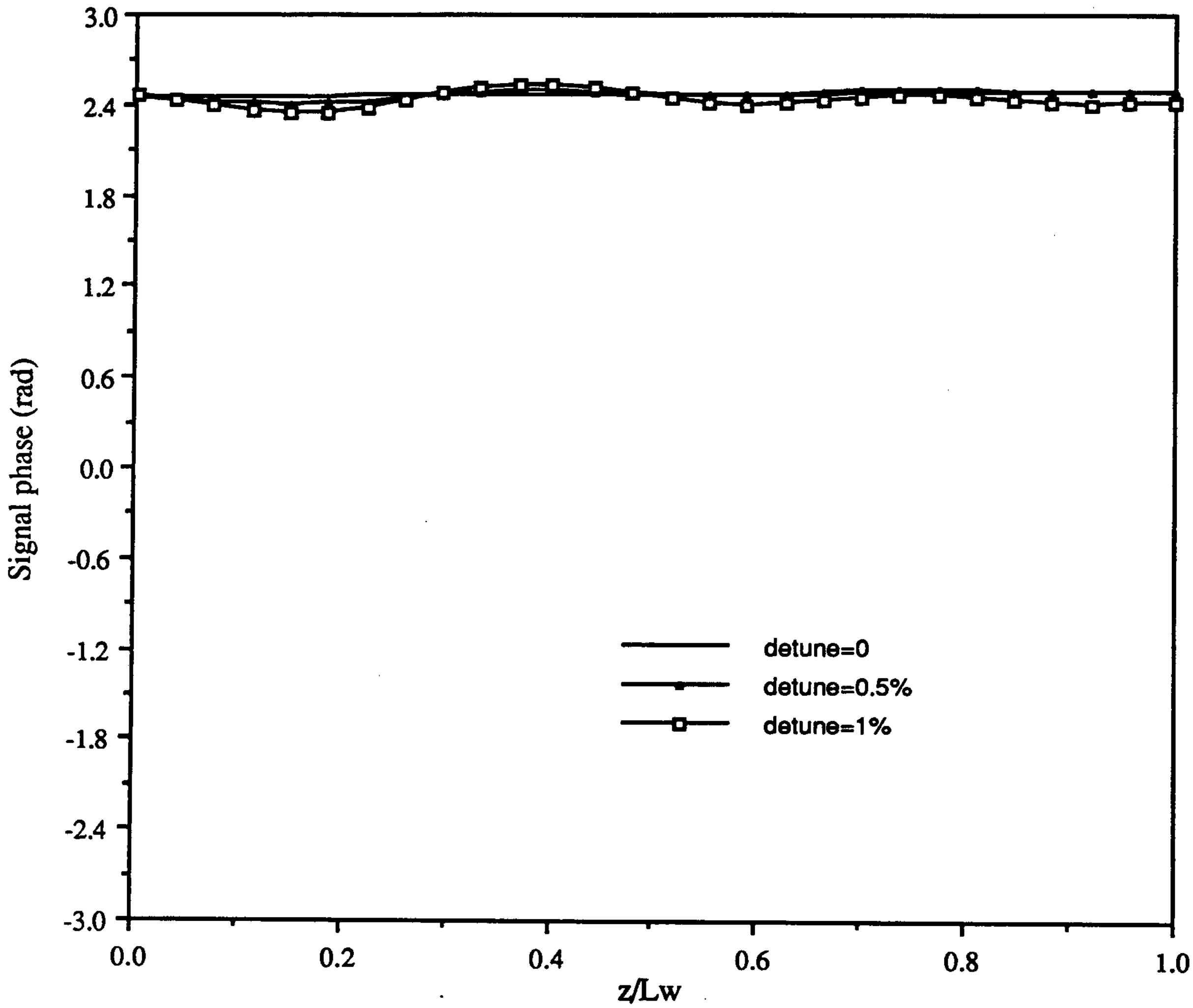
3.0
2.4
1.8
1.2
0.6
0.0
-0.6
-1.2
-1.8
-2.4
-3.0
Signal phase (rad)
0.0
0.2
0.4
0.6
0.8
1.0
z/Lw
detune=0
detune=0.5%
detune=1%

Fig. 4b

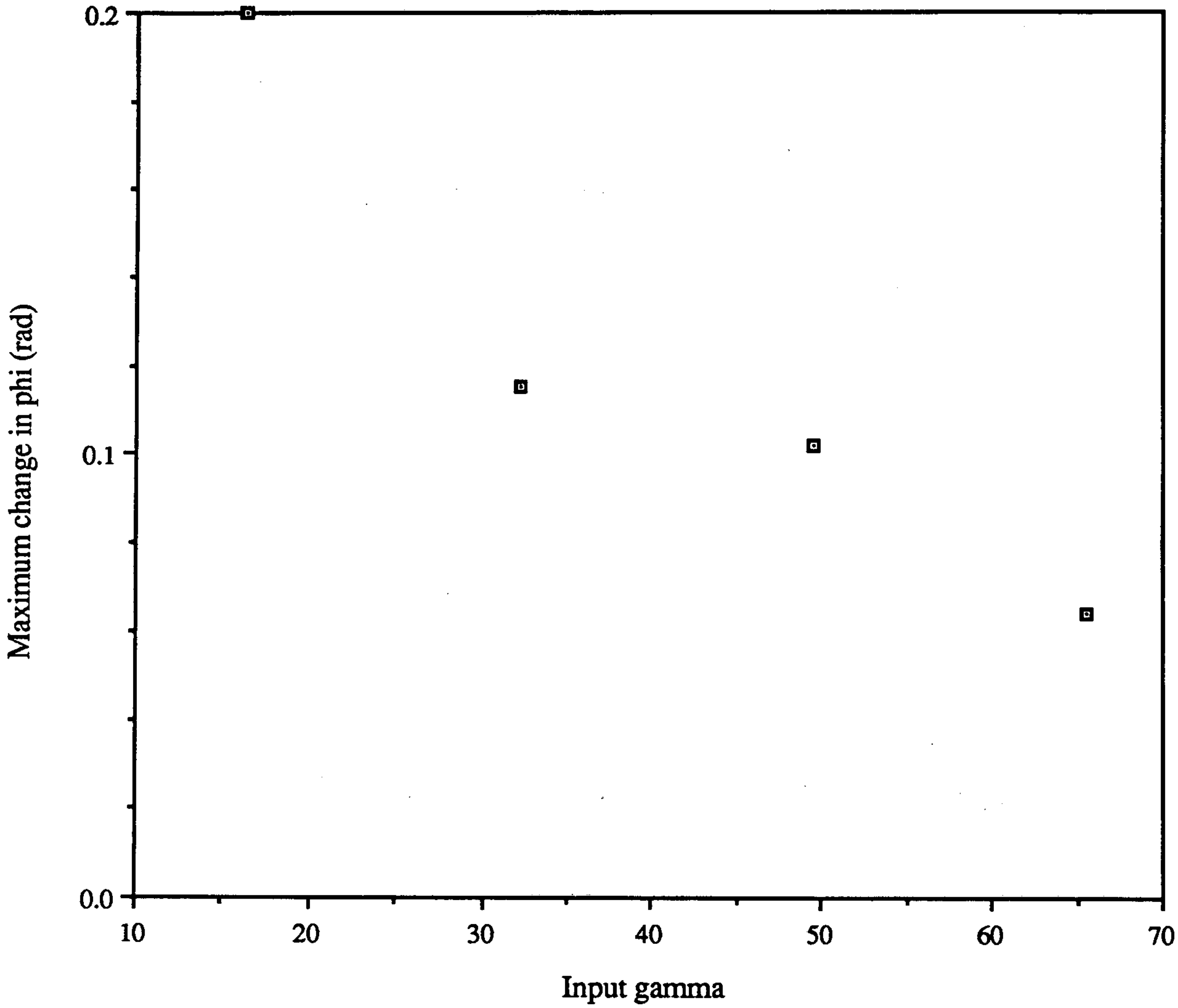
Maximum change in phi (rad)
0.2
0.1
0.0
10
20
30
40
50
60
70
Input gamma

Fig. 5

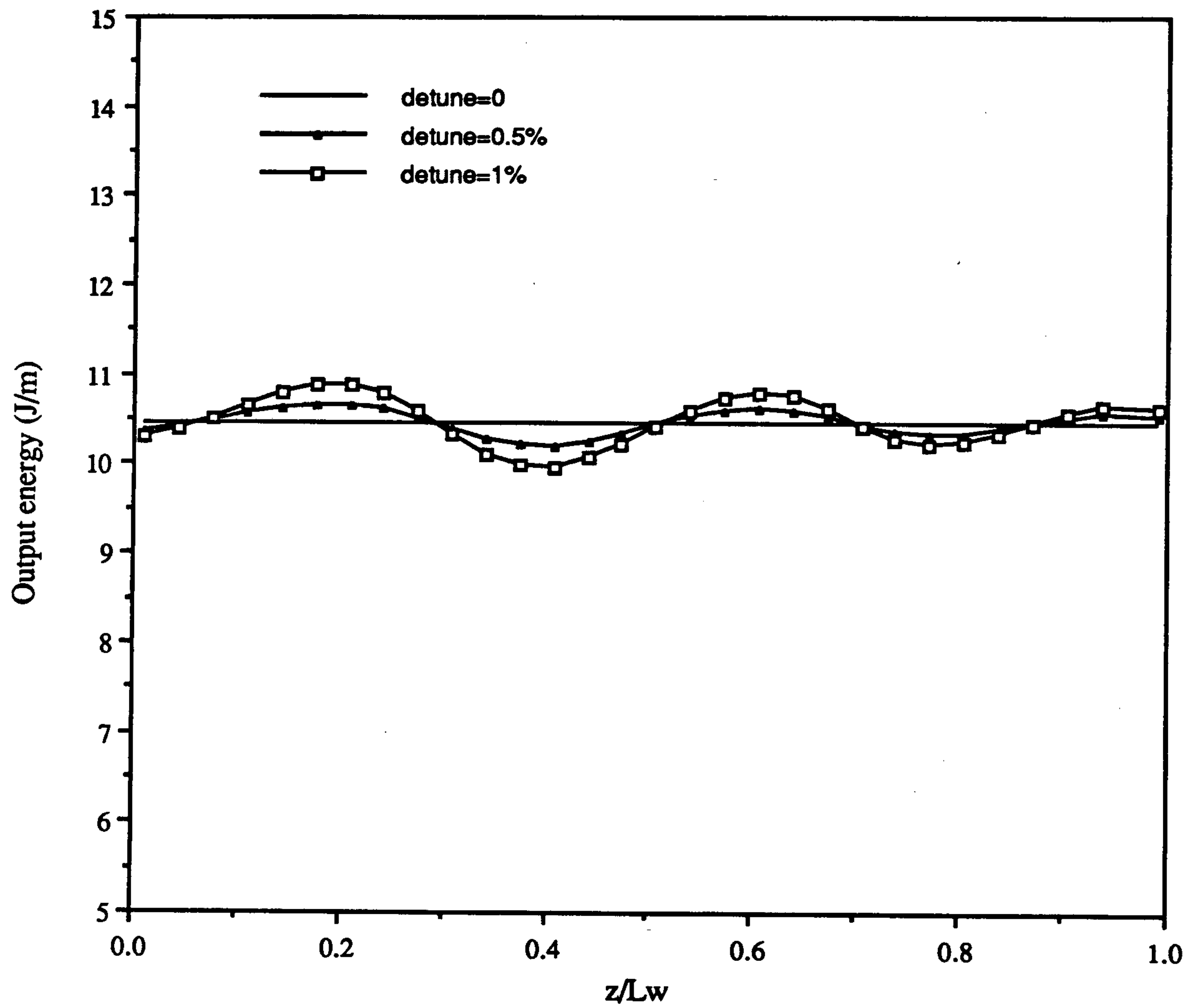

detune=0
detune=0.5%
detune=1%
Output energy (J/m)
15
14
13
12
11
10
9
8
7
6
5
0.0
0.2
0.4
0.6
0.8
1.0
z/Lw

Fig. 6a

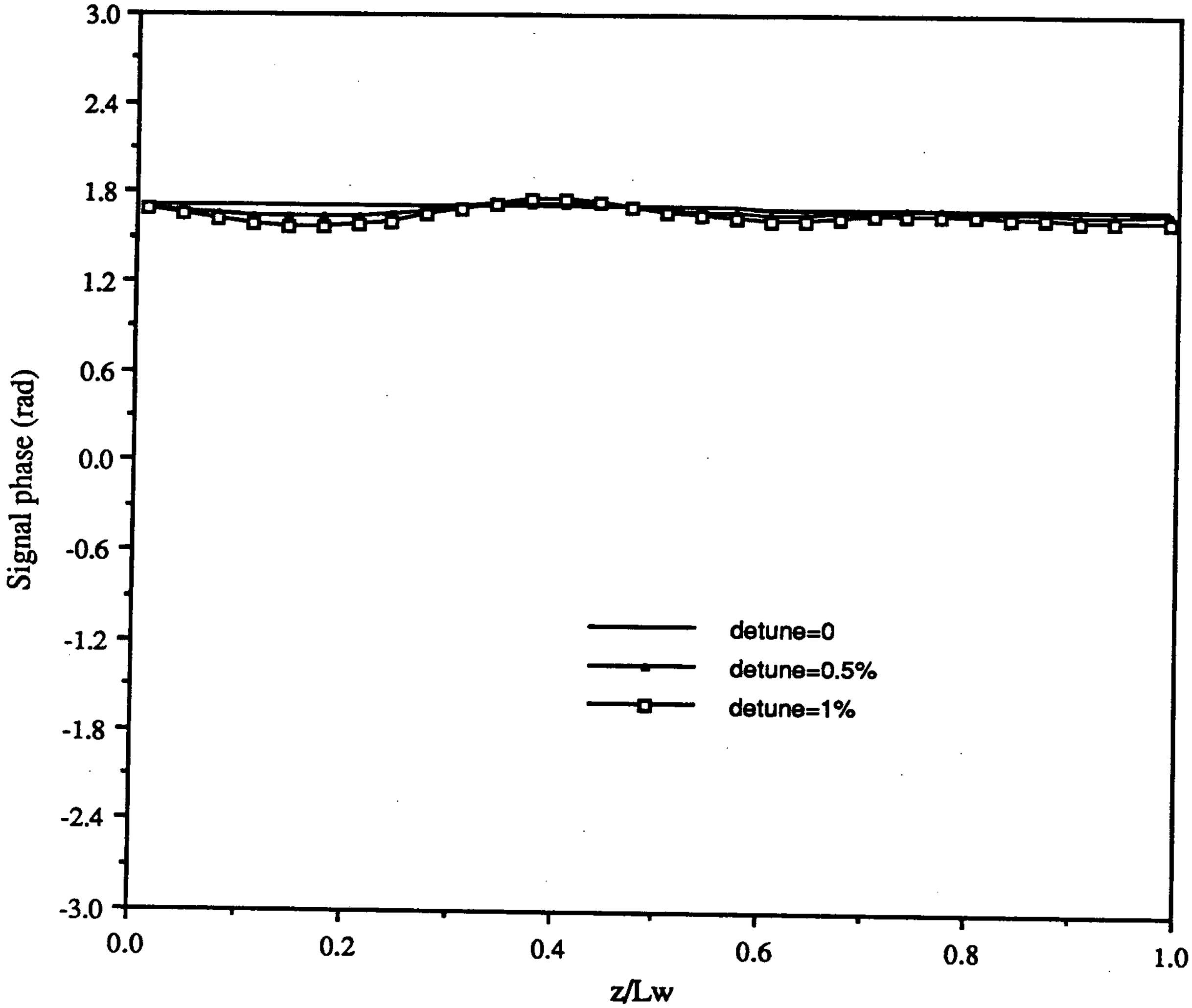

3.0
2.4
1.8
1.2
0.6
0.0
-0.6
-1.2
-1.8
-2.4
-3.0
Signal phase (rad)
0.0
0.2
0.4
0.6
0.8
1.0
z/Lw
detune=0
detune=0.5%
detune=1%

Fig. 6b

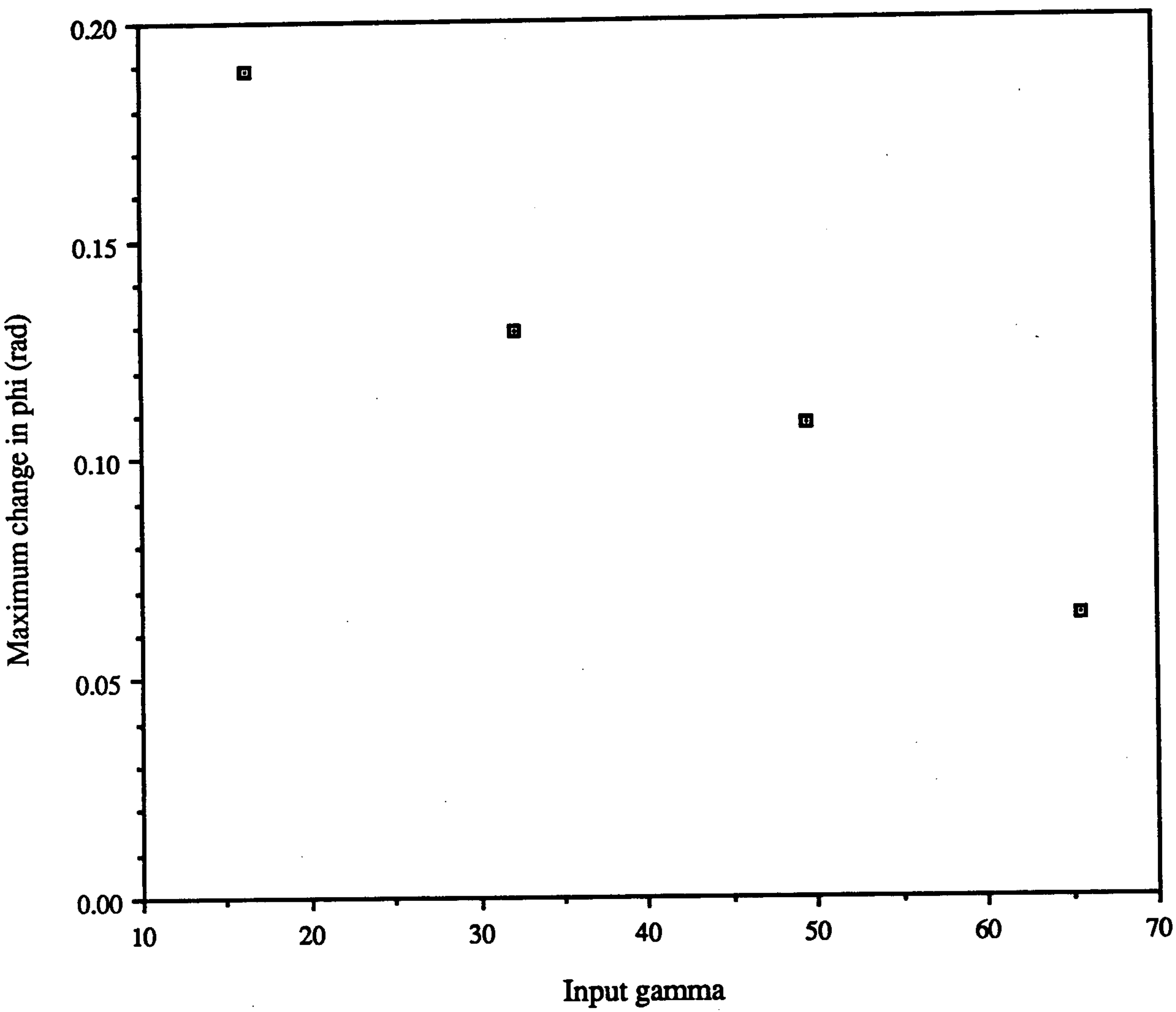
0.20
0.15
0.10
0.05
0.00
Maximum change in phi (rad)
10
20
30
40
50
60
70
Input gamma

Fig. 7

LAWRENCE BERKELEY LABORATORY
UNIVERSITY OF CALIFORNIA
TECHNICAL INFORMATION DEPARTMENT
BERKELEY, CALIFORNIA 94720